Korean J. Chem. Eng., **30**(7), 1386-1394 (2013)
DOI: 10.1007/s11814-013-0047-2

Effect of operating parameters on methanation reaction for the production of synthetic natural gas

Woo Ram Kang and Ki Bong Lee†

Department of Chemical and Biological Engineering, Korea University, Seoul 136-713, Korea
(*Received 14 December 2012 • accepted 1 April 2013*)

Abstract–Concerns about the depletion and increasing price of natural gas are generating interest in the technology of synthetic natural gas (SNG) production. SNG can be produced by the methanation reaction of synthesis gas obtained from coal gasification; this methanation reaction is the crucial procedure for economical production of SNG. We investigated the effect of operating parameters such as the reaction temperature, pressure, and feed compositions (H_2/CO and CO_2/CO ratios) on the performance of the methanation reaction by equilibrium model calculations and dynamic numerical model simulations. The performance of the methanation reaction was estimated from the CO conversion, CO to CH_4 conversion, and CH_4 mole fraction in the product gas. In general, a lower temperature and/or higher pressure are favorable for the enhancement of the methanation reaction performance. However, the performance becomes poor at low temperatures below 300 °C and high pressures above 15 atm because of limitations in the reaction kinetics. The smaller the amount of CO_2 in the feed, the better the performance, and an additional H_2 supply is essential to increase the methanation reaction performance fully.

Key words: Methanation, Methane, Synthetic Natural Gas, Operating Parameter

INTRODUCTION

The utilization of coal has long been known as the major factor contributing to pollution and global warming problems. However, there are many ongoing studies on clean coal technologies for the efficient control of the emission of pollutants from coal [1-3]. As a typical clean coal technology, coal-to-liquid technology converts coal into liquid fuels for transportation and boilers [4,5]. In addition, coal-to-synthetic natural gas (SNG) technology is attracting interest. SNG consists mostly of CH_4 (like natural gas), and therefore has similar properties to natural gas, which is clean and has a high energy conversion efficiency. In recent years, the demand for and dependence on natural gas has been increasing, and the price of natural gas is also increasing rapidly [6,7]. SNG production is expected to resolve the problems of the supply shortage and increasing price of natural gas. Coal is abundant, cheap, and distributed worldwide. SNG produced from coal is a stable fuel supply, and is cost-effective and environment-friendly. The additional major advantage of SNG is the potential to be able to use the existing gas infrastructure.

Fig. 1 shows a conventional process for SNG production from coal. When coal is heated at above 1,000 °C, synthesis gas containing CO, H_2, CO_2, and H_2O is produced from the gasifier. Up to now, many types of gasifier have been developed, and synthesis gas of various compositions can be obtained depending on the type of gasifier [8]. Synthesis gas compositions produced from typical commercial coal gasifiers are specified in Table 1 [9,10]. Synthesis gas has not only CO and H_2 as major components, but also several byproducts. For the production of SNG, byproducts such as sulfur and ammonia in the synthesis gas are mostly removed by the pretreatment process. Then, the refined synthesis gas enters the methanation reactor.

CO in the synthesis gas reacts with H_2 in a methanation reactor to produce CH_4 and H_2O at a temperature of about 300 °C. Therefore, high CO conversion is necessary for an efficient SNG production process and high SNG yield. Besides, the portion of CH_4 produced from CO is important because CO can be converted simultaneously to CO_2. The product gas from the methanation reaction, after water condensation, goes through purification processes for the production of high-purity CH_4.

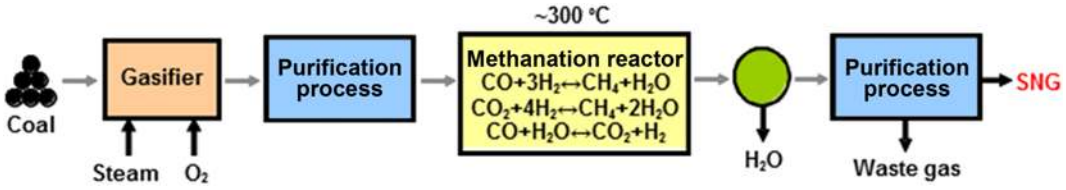

Fig. 1. Conventional process for the production of SNG from coal gasification.

†To whom correspondence should be addressed.
E-mail: kibonglee@korea.ac.kr

Table 1. Synthesis gas compositions produced from commercial coal gasifiers [9,10]

Gasifier	TRIG	BGL	Shell	Texaco	E-gas
CO (mol%)	39.7	54.3	57.2	34.4	42.0
H_2 (mol%)	28.5	29.7	29.0	33.5	33.2
CO_2 (mol%)	14.3	4.3	2.1	15.1	9.8
CH_4 (mol%)	4.3	5.9	0	0.1	0.4
H_2O (mol%)	12.6	0.2	3.6	14.3	12.2
Other gases[a] (mol%)	0.6	5.6	8.1	2.6	2.4
H_2/CO ratio	0.72	0.55	0.51	0.97	0.79
CO_2/CO ratio	0.36	0.08	0.04	0.44	0.23

[a]Other gases contain N_2, Ar, NH_3 and sulfur

In the 1970s, the oil crisis and a rapidly increasing demand for natural gas led to the development of SNG production processes based on fluidized bed operation and fixed bed operation [11-15]. However, there were some problems with the commercialization of these SNG production processes. First, there were technical problems in that the attrition of the catalyst and sintering occurred at the high reaction temperatures employed [16]. The high cost of SNG production was also a problem. Moreover, after a decade, the price of natural gas and oil stabilized owing to the discovery of new reserves, and most projects involving SNG synthesis were canceled.

During the last ten years, as the need and importance for efficient SNG production processes rose, research on SNG production technology has once again been progressing actively. GreatPoint Energy, US, has been developing a compact process called hydromethanation (bluegas™), which allows coal gasification and methanation simultaneously in one apparatus [17]. Research Triangle Institute, US, has also been developing a system for the production of both SNG and electricity from lignite or sub-bituminous coal [18, 19]. Furthermore, Arizona Public Service, US, has proposed the hydrogasification process, which can produce methane-containing syngas directly from the gasifier in the absence of a catalyst [20]. SNG synthesis from biomass and wood is now also under active development [21-24].

Though SNG production technologies have been developed for a long time, there have been few reports in the open literature of experimental and numerical simulation studies for understanding of the effects of operating conditions such as the temperature, pressure, and feed composition on the reactions for SNG production. Eisenlohr et al. [11] reported some brief results on the influence of reaction parameters on the methanation of coal gas to SNG on the basis of pilot-plant tests [11]. However, the investigated conditions of these parametric studies were limited to a narrow range because of the nature of pilot-plant experiments. A deep understanding of the effect of operating parameters on the methanation reaction performance is important for the development of an efficient and economical SNG production process.

In this study, the catalytic methanation reaction for SNG production was analyzed to elucidate the effects of the reaction temperature, pressure, and feed composition (H_2/CO and CO_2/CO ratios) by using equilibrium calculations and dynamic numerical model simulations. From the equilibrium model calculations, the dependence of the methanation reaction performance on these operating parameters was investigated on the basis of the synthesis gas composition from commercial coal gasification. A lower temperature, higher pressure, and/or lower CO_2 content in the feed are favorable for the enhancement of the methanation reaction performance. In particular, the H_2/CO ratio in the feed should be around 3 in order to maximize the methanation reaction performance. In the dynamic numerical model simulation, the performance of the methanation reaction becomes poor at low temperatures below 300 °C and high pressures above 15 atm owing to limitations in the reaction kinetics.

THEORETICAL MODELING

1. Equilibrium Model

In the catalytic methanation reaction, the synthesis gas produced by coal gasification is converted into the product gas containing CH_4. The major chemical reactions that take place in the methanation reactor can be described by the following three equations:

CO methanation reaction

$$CO+3H_2 \leftrightarrow CH_4+H_2O \qquad \Delta H_{298\,K}=-206\ \text{kJ/mol} \tag{1}$$

Water gas shift reaction

$$CO+H_2O \leftrightarrow CO_2+H_2 \qquad \Delta H_{298\,K}=-41\ \text{kJ/mol} \tag{2}$$

CO_2 methanation reaction

$$CO_2+4H_2 \leftrightarrow CH_4+2H_2O \qquad \Delta H_{298\,K}=-165\ \text{kJ/mol} \tag{3}$$

The methanation reactions are controlled by the thermodynamic equilibrium. The CO methanation reaction (reaction 1) is a primary and highly exothermic reaction. The water gas shift reaction (reaction 2) is mildly exothermic, and the CO_2 methanation reaction (reaction 3) is dependent on reactions 1 and 2. Starkey et al. [25] found experimentally that the CO_2 methanation reaction did not occur as long as the concentration of CO was greater than a few hundred ppm [25]. The equilibrium constants of the three reactions can be represented as follows:

$$K_1(T)=\frac{(Y_{CH_4})(Y_{H_2O})}{(Y_{CO})(Y_{H_2})^3}P^{-2} \tag{4}$$

$$K_2(T)=\frac{(Y_{CO_2})(Y_{H_2})}{(Y_{CO})(Y_{H_2O})} \tag{5}$$

$$K_3(T)=K_1(T)/K_2(T) \tag{6}$$

where Y_j is the gas-phase mole fraction of component j, P is the total pressure, and T is the temperature. The equilibrium constants of the reactions can also be expressed as a function of temperature [26]:

$$K_1(T)=\exp(0.2513Z^4-0.3665Z^3-0.5810Z^2+27.1337Z-3.2770),\ \text{atm}^{-2} \tag{7}$$

$$K_2(T)=\exp(-0.29353Z^3+0.63508Z^2+4.1778Z+0.31688) \tag{8}$$

where Z=(1000−T)/T (T in Kelvin).

When the reaction temperature and pressure are fixed in a batch reactor and the feed gas contains CO, CO_2, and H_2 only, the equilibrium compositions of the product gas can be represented as follows:

$$Y_{CH_4}=\frac{x}{\alpha+\beta+\gamma-2x} \tag{9}$$

$$Y_{CO_2}=\frac{\beta-y}{\alpha+\beta+\gamma-2x} \tag{10}$$

$$Y_{H_2O}=\frac{x+y}{\alpha+\beta+\gamma-2x} \tag{11}$$

$$Y_{H_2}=\frac{\gamma-3x-y}{\alpha+\beta+\gamma-2x} \tag{12}$$

$$Y_{CO}=\frac{\alpha-x+y}{\alpha+\beta+\gamma-2x} \tag{13}$$

where α, β, and γ are the numbers of moles of initial CO, CO_2, and H_2, respectively, in the reactor, x is the number of moles of reacted CO in reaction 1, and y is the number of moles of reacted CO_2 in reaction 2. Using Eqs. (4)-(13), the relation between the equilibrium constants and equilibrium compositions of product gas can be derived as follows:

$$K_1(T)=\frac{x(x+y)(\alpha+\beta+\gamma-2x)^2}{(\alpha-x+y)(\gamma-3x-y)^3}P^{-2} \tag{14}$$

$$K_2(T)=\frac{(\beta-y)(\gamma-3x-y)}{(\alpha-x+y)(x+y)} \tag{15}$$

Consequently, equilibrium product composition is determined by the reaction temperature, pressure, and feed composition. The equilibrium state, which ideally is reached in the methanation reactions, was calculated to elucidate the effects of the reaction temperature, pressure, and feed composition on the methanation performance.

2. Dynamic Numerical Model

CO conversion, CO to CH_4 conversion, and equilibrium mole fractions based on the abovementioned equilibrium model were calculated with the assumption that the reactions were fast enough to reach their equilibrium states. However, in the actual reaction, the reaction rate can limit the reaction performance. Therefore, a kinetic model should be considered to account for the performance limitation caused by the reaction rates. The following empirical but analytical expressions describing the relevant methanation kinetics for a commercial nickel on alumina catalyst were reported by Xu and Froment [27]. This kinetic model describes experimental results in the literature well, and has been used widely [28-30].

CO methanation reaction

$$r_1=\frac{k_1}{p_{H_2}^{2.5}}[p_{CH_4}p_{H_2O}-p_{H_2}^3p_{CO}K_1]/A^2 \tag{16}$$

Water gas shift reaction

$$r_2=\frac{k_2}{p_{H_2}}\left[p_{CO}p_{H_2O}-\frac{p_{H_2}p_{CO_2}}{K_2}\right]/A^2 \tag{17}$$

CO_2 methanation reaction

$$r_3=\frac{k_3}{p_{H_2}^{3.5}}\left[p_{CH_4}p_{H_2O}^2-\frac{p_{H_2}^4p_{CO_2}K_1}{K_2}\right]/A^2 \tag{18}$$

where $A=1+\delta_{CO}p_{CO}+\delta_{H_2}p_{H_2}+\delta_{CH_4}p_{CH_4}+\delta_{H_2O}p_{H_2O}/p_{H_2}$, r_i and k_i are the reaction rate and rate constant of reaction i, respectively, p_j is the partial pressure of component j, and δ_j is the surface adsorption parameter in equilibrium, which depends on temperature [31].

A conventional shell-and-tube-type heat-exchanger was assumed as the methanation reactor vessel in the numerical simulation study. The tube side (diameter=d_c, cross-sectional area=A, length=L_c) of the heat-exchanger is packed with a methanation catalyst (bulk density=ρ_b, heat capacity=c_{ps}, void fraction=ε). Superheated steam is passed in the shell side (cross-flow) to maintain the outside tube walls at a constant temperature (T_w) at all times. The well-known model of continuous stirred tank reactors (CSTRs) in series was adapted for the dynamic simulations [32]. The key model assumptions included (i) ideal gas behavior, (ii) instantaneous thermal equilibrium between the gas and solid inside the reactor tube, and (iii) the absence of axial dispersion and column pressure drop. The algebraic equation and ordinary differential equations of the model representing (i) the transient component and overall mass balances, and (ii) the transient energy balance including heat transfer from the shell side to the tube side (overall heat transfer coefficient=U_o) at any time (t), are given below [33]:

Overall molar balance in the gas phase

$$N^{out}A=N^{in}A-\rho_bV_{stage}\left[\sum_i\sum_j r_{i,j}\right]-\frac{dn_t}{dt} \tag{19}$$

Component molar balance in the gas phase

$$\frac{dY_j}{dt}=\frac{1}{n_t}\left[N_{in}A(Y_j^{in}-Y_j)+\rho_bV_{stage}\left\{\sum_j r_{i,j}\right\}-Y_j\rho_bV_{stage}\left\{\sum_i\sum_j R_{i,j}\right\}\right] \tag{20}$$

Energy balance

$$\eta\rho_bV_{stage}c_{ps}\frac{dT}{dt}=N^{in}Ac_{pg}(T^{in}-T)-\rho_bV_{stage}\left[\sum_i\Delta H_ir_i\right]+\pi d_cL_{stage}U_o(T_w-T) \tag{21}$$

Ideal gas law

$$n_t=\frac{V_{stage}\varepsilon P}{RT} \tag{22}$$

where c_{pg} is the heat capacity of the gas phase, ΔH_i is the heat of reaction i, N is the total gas flux, n_t is the total number of moles in the gas phase, and r_i is the rate of reaction i. L_{stage} and V_{stage} are the length and volume of a CSTR stage, respectively, R is the gas constant, and η (=1.2) is a factor to account for the heat capacity of the heat-exchanger tube and body. In the dynamic numerical simulations, the following reactor parameters were kept constant.

Tube (column) inside diameter (d_c): 1.73 cm
Tube (column) length (L_c): 50 cm
Bulk density (ρ_b): 0.824 g/cm^3

The above equations were solved simultaneously by the Matlab function ODE23s, which is a variable-order solver based on the numerical differentiation formulas. The methanation performance was estimated from the CO conversion, CO to CH_4 conversion, and CH_4 mole fraction in the product gas, as defined below:

(CO conversion)=(reacted CO)/(CO in feed)
(CO to CH_4 conversion)=(produced CH_4)/(reacted CO)
(CH_4 mole fraction)=(amount of CH_4 in product gas)/(total amount of components in product gas)

In the methanation reactions, CO in feed can react to form either

CH_4 or CO_2. To show how much CO is selectively converted into CH_4, (CO to CH_4 conversion) is used for a performance indicator.

EXPERIMENTAL

The methanation reaction experiment was carried out using a conventional catalytic fixed bed reactor. The middle of the fixed bed reactor was packed with 1 g of catalyst pellets containing 46% nickel supported on alumina (Sud-Chemie). The feed gas was a mixture of CO, H_2, and N_2 (carrier gas) with a H_2/CO ratio of 2.5, and N_2/CO ratio of 4.3, and the flow rate was fixed at 1.32 mmol/(min·cm^2). The methanation reaction experiment was performed at 1 atm and 275 °C. Before the methanation reaction experiment was started, the catalytic reactor was filled with a H_2/N_2 mixture gas. The effluent gas from the reactor passed through a condenser to remove byproduct H_2O, and the composition of the dried product gas was analyzed by gas chromatography (Agilent Technologies-3000A) apparatus equipped with two thermal conductivity detectors. One detector analyzed CH_4, CO, and H_2 with He as the carrier gas, and CO_2 was analyzed in another detector with Ar as the carrier gas.

RESULTS AND DISCUSSION

1. Equilibrium Model Calculation (Based on Feed Composition from Coal Gasifier)

The effects of parameters such as the reaction temperature, pressure, and feed composition were investigated by varying a particular parameter while maintaining the other parameters constant, as in the base case below. The synthesis gas composition produced from the Shell gasifier in Table 1 was considered as the feed composition, and the synthesis gas was assumed to be purified through purification processes.

T=300 °C, P=10 atm, H_2/CO (γ/α)=0.51, CO_2/CO (β/α)=0.04

1-1. Effect of Reaction Temperature

Fig. 2 shows the effect of the reaction temperature on the CO conversion, CO to CH_4 conversion, and CH_4 mole fraction in the product gas from the methanation reaction. Generally, in the exothermic methanation reaction, a lower temperature is favorable for increasing both the CO conversion and CH_4 mole fraction in the product gas (as seen at temperatures above 500 °C). This can also be expected from the change in equilibrium constants as a function of temperature (Fig. 3) [26]. The equilibrium constants of both the exothermic reactions (1 and 2) decrease with increasing temperature. However, in the reaction temperature range 100-500 °C, the CO conversion and CH_4 mole fraction in the product gas stay almost constant with changing reaction temperature. This is because the performance of the methanation reaction is limited by other parameters, resulting in a weak dependence on temperature below 500 °C. Interestingly, the CO to CH_4 conversion increases with increasing temperature above 500 °C. It indicates that CH_4 production from CO by reaction 1 becomes more dominant than CO_2 production from CO by reaction 2, while both reactions are simultaneously retarded in the high temperature region.

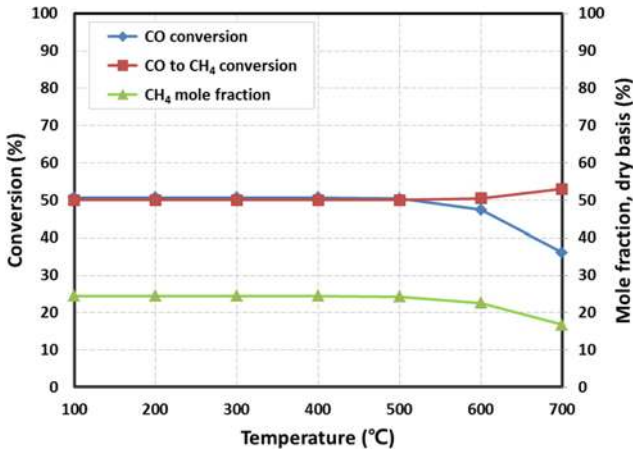

Fig. 2. Effect of reaction temperature on the performance of the methanation reaction (based on equilibrium model calculations).

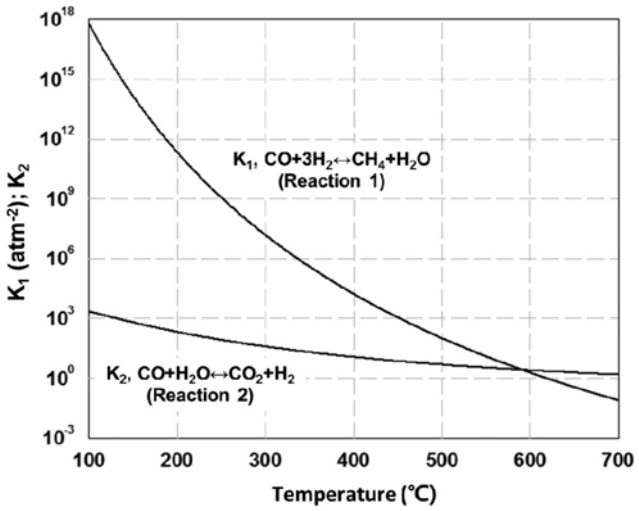

Fig. 3. Equilibrium constants (K_1 and K_2) at different temperatures.

1-2. Effect of Reaction Pressure

As shown in Fig. 4, the CO conversion and CH_4 mole fraction in the product gas increase slightly with increasing pressure in the low-pressure range of 0.01-1 atm. The effect of the reaction pres-

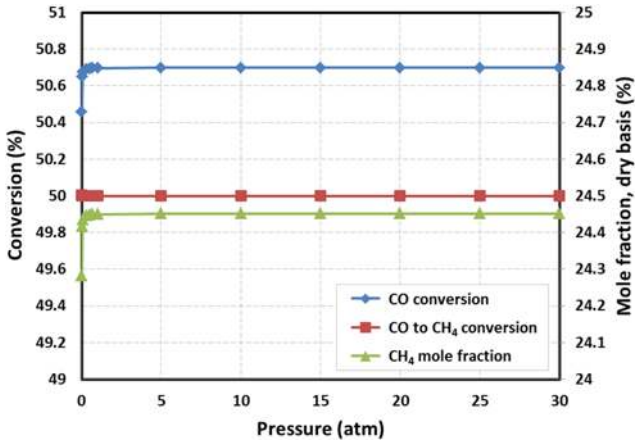

Fig. 4. Effect of reaction pressure on the performance of the methanation reaction (based on equilibrium model calculations).

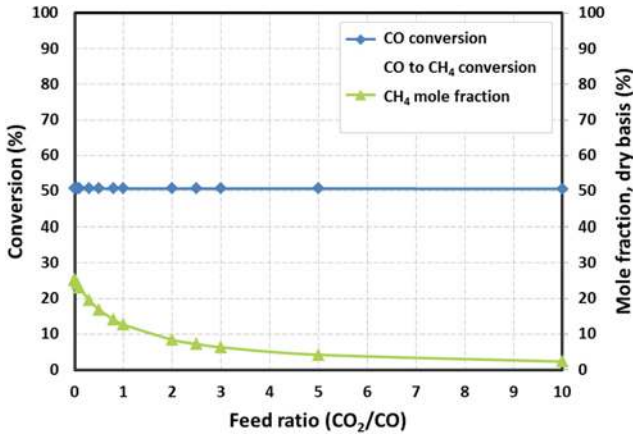

Fig. 5. Effect of CO_2/CO ratio in feed gas on the performance of the methanation reaction (based on equilibrium model calculations).

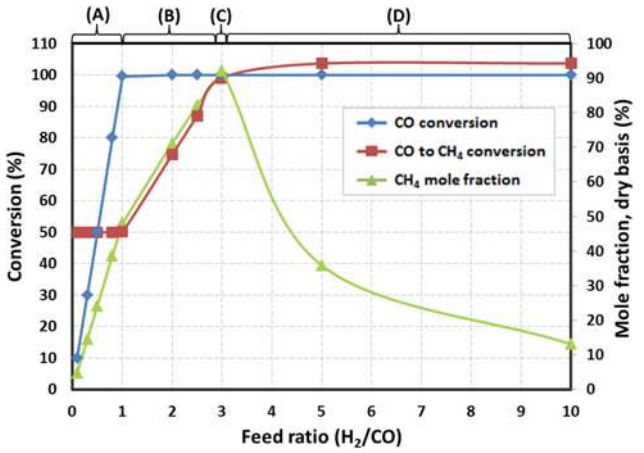

Fig. 6. Effect of H_2/CO ratio in feed gas on the performance of the methanation reaction (based on equilibrium model calculations).

sure can be predicted from the relation between the equilibrium constants and the pressure. In reaction 1, with increasing pressure, the equilibrium constant decreases, shifting the equilibrium composition to the product side (Eq. (14)). However, the equilibrium constant of reaction 2 is not affected by the pressure, because the number of moles of reactant is the same as that of product (Eq. (15)). At pressures over 1 atm, the CO conversion and CH_4 mole fraction in the product gas are not affected by the reaction pressure. Over the pressure range studied, the CO to CH_4 conversion remains constant at 50%.

1-3. Effect of CO_2/CO Ratio in Feed Gas

As shown in Table 1, the synthesis gases produced from coal gasifiers contain various CO_2 concentrations. The effect of the CO_2/CO ratio in the feed is shown in Fig. 5. Regardless of the CO_2/CO ratio, the CO conversion and CO to CH_4 conversion remain constant at 50%, indicating that the CO_2 concentration has little effect on the CO conversion under these conditions. The CO_2 in the initial feed hardly participates in the methanation reactions, and remains in the final equilibrium-state product. Consequently, the CH_4 mole fraction in the product gas decreases with increasing CO_2/CO ratio.

1-4. Effect of H_2/CO Ratio in Feed Gas

Fig. 6 shows that the performance of the methanation reaction changes significantly with the H_2/CO ratio. The investigated conditions can be divided into four regions according to the effects of the H_2/CO ratio, and the results of the equilibrium calculations are shown in Table 2. When the amount of H_2 in the feed is quite small compared to the stoichiometric ratio of H_2 and CO in reaction 1, 3 : 1 (region A, containing the base case), the CO conversion and CH_4 mole fraction in the product gas increase significantly with increasing H_2/CO ratio. On the other hand, the CO to CH_4 conversion remains at 50% in region A. This means that CO is converted simultaneously into both CH_4 and CO_2. As CH_4 is produced from the CO methanation reaction, H_2O is also produced as a byproduct. Then, the produced H_2O can react with CO to produce CO_2, resulting in an increased amount of CO_2 in the product. When the H_2/CO ratio is 0.5 (Table 2), the amount of CO_2 produced is as much as that of CH_4. For this reason, the degree of increase in the CO conversion is about double that in the CH_4 mole fraction in the product gas, as shown in Fig. 6. When the H_2/CO ratio is more than 1 (region B), CO conversion is greater than 99% because there is enough H_2 for the methanation reactions. Nevertheless, when the H_2/CO ratio is 1 (Table 2), the CO to CH_4 conversion and CH_4 mole fraction in the product gas are just about 50%; this is not high enough for the SNG production process, and excessive CO_2 is produced as a byproduct. The CO to CH_4 conversion and CH_4 mole fraction in the product gas can increase further with increasing H_2/CO ratio. As the H_2/CO ratio increases and becomes closer to 3, the stoichiometric ratio of H_2 and CO in reaction 1, the CO to CH_4 conversion and CH_4 mole fraction in the product gas are increased remarkably. When the H_2/CO ratio is the same as the stoichiometric ratio of H_2 and CO in reaction 1 (region C), most CO is converted into CH_4, and the CO to CH_4 conversion is about 99%. Moreover, the CH_4 mole fraction reaches the maximum of 92%, as seen in Table 2. When excessive H_2 is present in the feed (region D), the CO conversion and CO to CH_4 conversion remain at their maximum values. In particular, CO_2 in the feed is converted into CO through reaction with excess H_2, and the produced CO is further converted to CH_4, and hence, the CO to CH_4 conversion exceeds 100%. However, in region

Table 2. Results of equilibrium model calculations for methanation reaction at different H_2/CO ratios

H_2/CO ratio in feed	Dry-basis equilibrium mol composition in product (%)				CO conversion (%)	CO to CH_4 conversion (%)
	CO	CO_2	CH_4	H_2		
0.5	48.23	27.66	24.11	3.4 ppm	50.00	50.00
1	0.40	51.46	48.09	0.05	99.59	50.01
3	43.9 ppm	4.31	92.10	3.59	99.995	99.04
5	~0	~0	35.87	64.13	~100	103.67

D, the CH_4 mole fraction in the product gas decreases with increasing H_2/CO ratio because most of the H_2 still remains in the product gas, as shown in Table 2. The above results clearly show that the H_2/CO ratio is the most important of the operating parameters. In particular, when the H_2/CO ratio is 3, the methanation performance is high enough for SNG production.

2. Equilibrium Model Calculation (Based on the Modified Feed Composition)

The low and restricted performance of the methanation reaction in the previous results for the effects of the reaction temperature, pressure, and CO_2/CO ratio appears to be caused by the deficient amount of H_2 for the methanation reaction. For the full elucidation of the effect of the reaction temperature, pressure, and CO_2/CO ratio, we did the equilibrium model calculations again with the modified feed composition below. We assumed that additional H_2 was supplied to the feed, and the H_2/CO ratio of 3 was chosen for the base case.

T=300 °C, P=10 atm, H_2/CO (γ/α)=3, CO_2/CO (β/α)=0.04

2-1. Effect of Reaction Temperature (H_2/CO Ratio=3)

As seen in Fig. 7, the CO conversion, CO to CH_4 conversion, and CH_4 mole fraction in the product gas increase sharply over the investigated temperature range, compared to the result in Fig. 2 when H_2/CO ratio is 0.51. This increase is achieved with increasing H_2/CO ratio to 3. Because the exothermic methanation reaction is unfavorable at high temperatures, the CO conversion and CH_4 mole fraction in the product gas decrease with increasing reaction temperature. From 100-300 °C, the CO conversion and CO to CH_4 conversion are both over 99%, and the CH_4 mole fraction in the product gas is greater than 90%.

2-2. Effect of Reaction Pressure (H_2/CO Ratio=3)

Fig. 8 shows the effect of the reaction pressure on the performance of the methanation reaction when the H_2/CO ratio is 3. Generally, the methanation performance is enhanced with increasing reaction pressure. The effect of reaction pressure is clear in the low pressure range below 1 atm, and is hardly observed above 15 atm.

2-3. Effect of CO_2/CO Ratio in Feed Gas (H_2/CO Ratio=3)

In contrast to Fig. 5, the changes in the CO conversion and CO to CH_4 conversion as a function of CO_2/CO ratio can be observed

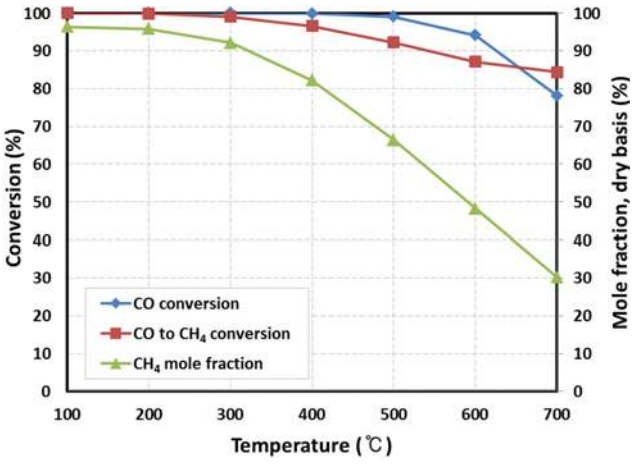

Fig. 7. Effect of reaction temperature on the performance of the methanation reaction (based on equilibrium model calculations, H_2/CO ratio=3).

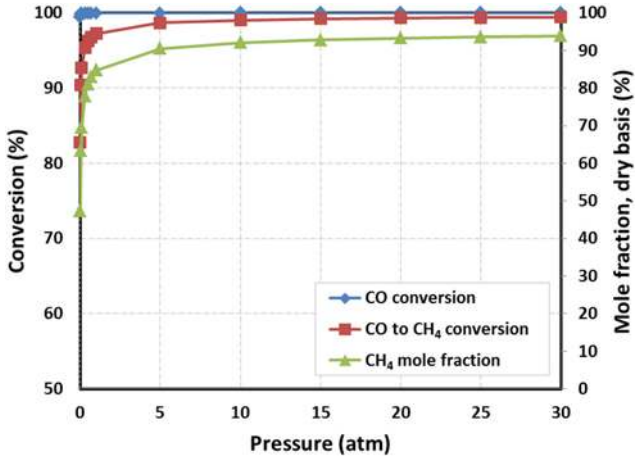

Fig. 8. Effect of reaction pressure on the performance of the methanation reaction (based on equilibrium model calculations, H_2/CO ratio=3).

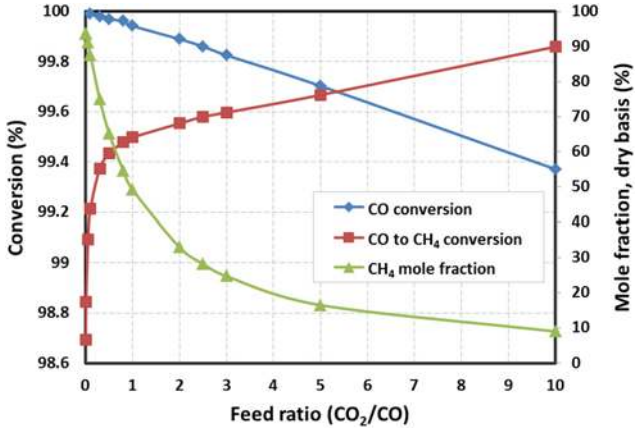

Fig. 9. Effect of CO_2/CO ratio in feed gas on the performance of the methanation reaction (based on equilibrium model calculations, H_2/CO ratio=3).

clearly in Fig. 9 for the H_2/CO ratio of 3. When the CO_2/CO ratio increases, the reverse water gas shift reaction can occur, and the CO concentration increases. The increased amount of CO enhances the CO methanation reaction. As a result, the CO conversion decreases slightly, but the CO to CH_4 conversion increases with increasing CO_2/CO ratio (Fig. 9). Despite these effects, the CO conversion and CO to CH_4 conversion are above 98% over the investigated range. It appears that CO_2 hardly participates in the methanation reaction and remains in the product gas. As a result, as the CO_2/CO ratio increases, the CH_4 mole fraction in the product gas decreases. For a high CH_4 concentration in the product gas, the CO_2 concentration should be minimized in the feed.

3. Comparison of Experimental Data and Simulation Results

Before simulations were conducted using the dynamic numerical model, the dynamic numerical model was validated through comparison with experimental data (Fig. 10). The effluent gas compositions from the methanation reaction are shown in Fig. 10. The time, t, was normalized by the breakthrough time, t_b, for the equilibrium-state concentration of 50% CH_4. The effluent gas from the reactor initially consists mostly of H_2. When the product gas from the metha-

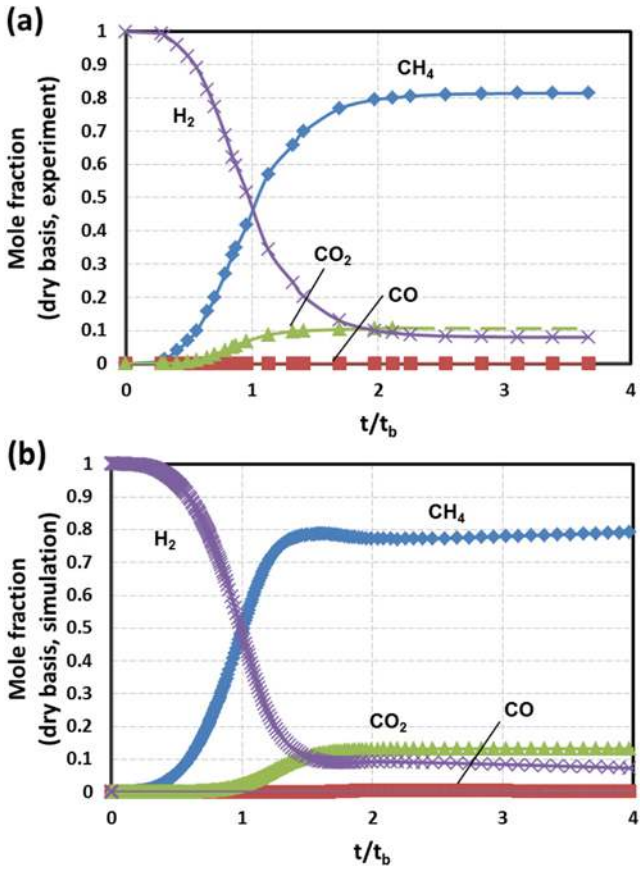

Fig. 10. Effluent gas compositions from methanation reaction: (a) experiment and (b) dynamic numerical simulation (T=275 °C, P=1 atm, H_2/CO=2.5, N_2/CO=4.29, N_{in}=1.32 mmol/(min·cm^2), catalyst=1 g).

nation reaction comes out from the reactor, the CH_4 concentration increases sharply and then reaches the equilibrium state (Fig. 10(a)). A reasonable CO conversion of ~99% and CH_4 mole fraction of ~80% were obtained experimentally. Identical reaction conditions were applied in the dynamic numerical simulations. However, the simulated reaction based on the kinetic model of Xu and Froment [27] appeared to be slower than that shown by the experimental data. The rate constants in the kinetic model of Xu and Froment were estimated based on the experimental date performed at the temperature ranging from 300 to 500 °C. Different experimental conditions could cause discrepancy in rate constants. To obtain similar dynamic behavior between the experiment and simulation, the reaction rate constants were fine-tuned. With modified rate constants ($100\times k_1$ and $10\times k_2$), good agreement between the numerical simulation results and experimental data was observed (Fig. 10).

4. Dynamic Numerical Model Simulation

Sufficiently fast reactions were assumed in the equilibrium model calculations. However, in the actual reaction, the reaction kinetics can limit the reaction performance. To explain the effect of the reaction kinetics, we performed a numerical simulation based on the dynamic model and compared its results with the previous equilibrium model calculations. In the dynamic numerical model simulation, the catalytic reactor was assumed to be initially filled with CH_4 in order to maintain high CH_4 purity in the product. The CO conversion, CO to CH_4 conversion, and CH_4 mole fraction in the product gas were obtained after a sufficient length of time, when the methanation reaction reached a steady state. The base case in the dynamic numerical model simulation was chosen as follows:

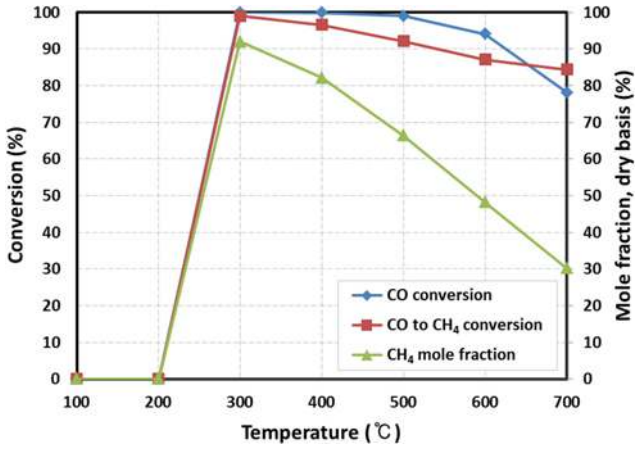

Fig. 11. Effect of reaction temperature on the performance of the methanation reaction (based on dynamic numerical model simulation).

T=300 °C, P=10 atm, H_2/CO (γ/α)=3, CO_2/CO (β/α)=0.04, N_{in}=30 mmol/(min·cm^2)

4-1. Effect of Reaction Temperature

Fig. 11 shows a similar effect of reaction temperature to that shown in Fig. 7 at temperatures above 300 °C. The CO conversion, CO to CH_4 conversion, and CH_4 mole fraction in the product gas decrease with increasing temperature in the temperature range 300-700 °C because the reactions are exothermic. However, because of kinetic limitations at low temperatures, no methanation reactions occur between 100 and 200 °C, and the reaction performance increases significantly between 200 and 300 °C. The methanation reaction performance is controlled by the reaction rate at low temperatures and by thermodynamic equilibrium at high temperatures. Considering the reaction rate and thermodynamic equilibrium, the maximum performance is achieved at about 300 °C.

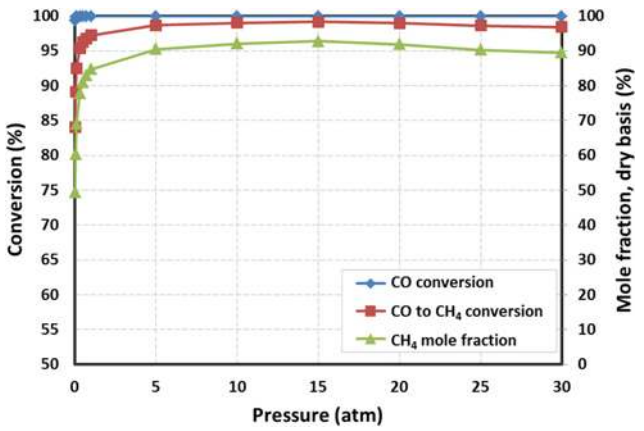

Fig. 12. Effect of reaction pressure on the performance of the methanation reaction (based on dynamic numerical model simulation).

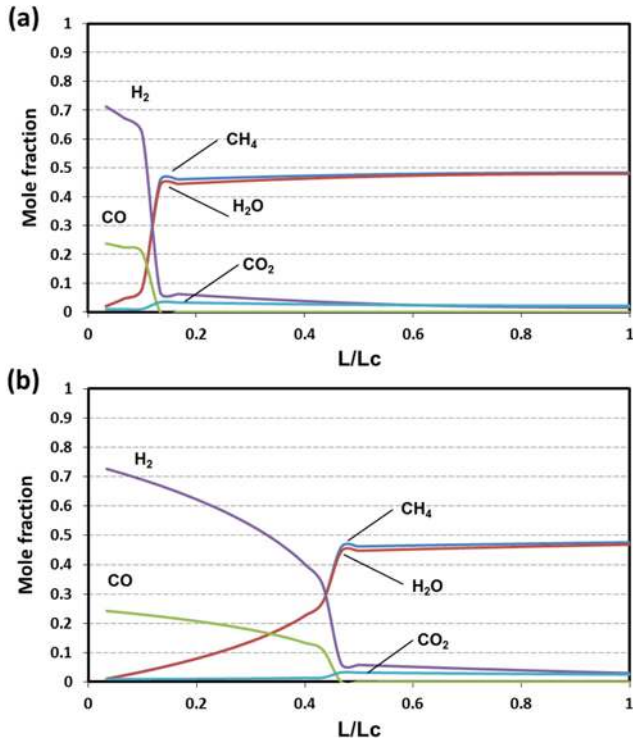

Fig. 13. Component mole fraction inside the methanation reaction column at (a) 15 atm and (b) 30 atm (runtime=300 min).

4-2. Effect of Reaction Pressure

Fig. 12 shows a similar effect of reaction pressure to that shown in Fig. 8, except in terms of the CO to CH_4 conversion and CH_4 mole fraction in the product gas at high pressures. Generally, the performance of the methanation reaction increases with increasing reaction pressure. However, the CH_4 mole fraction in the product gas decreases slightly at high pressures above 15 atm. This is caused by the slowed reactions at high pressures. Fig. 13 shows the component mole fraction inside the catalytic reactor in the methanation reaction after a sufficient length of time (300 min), when the methanation reaction reaches a steady state. When the pressure increases from 15 atm (Fig. 13(a)) to 30 atm (Fig. 13(b)), the concentration column profiles shift to the end of the reactor, indicating that the reaction rate is delayed at the higher pressure. As the reaction rate decreases, the methanation reaction cannot reach its equilibrium state in the catalytic reactor, and its performance is lower than that of the equilibrium reaction. The slow decrease of CO_2 and H_2 concentrations in the rear part of the reactor indicates that reaction 3 happens very slowly in that area. As the area where slow reaction 3 dominantly happens decreases, additional CH_4 production by reaction 3 can be reduced. This is thought to cause a slight decrease of CO to CH_4 conversion and CH_4 mole fraction in Fig. 12 at high pressure regions.

The effects of the H_2/CO and CO_2/CO ratios in the dynamic numerical model simulations are not shown because the results are the same as those found through the equilibrium calculations. The methanation reaction rate is independent of the feed compositions.

CONCLUSIONS

The effects of various operating parameters on the methanation reaction for SNG production were investigated by equilibrium model calculations and dynamic numerical model simulations. The parameters studied were the reaction temperature, pressure, and feed compositions (H_2/CO and CO_2/CO ratios). The performance of the methanation reaction was estimated from the CO conversion, CO to CH_4 conversion, and CH_4 mole fraction in the product gas.

The methanation reaction is exothermic, and the total stoichiometric number of moles of products is less than the number of moles of reactants. Therefore, the performance of the methanation reaction is, in general, improved as the reaction temperature decreases and/or the reaction pressure increases. However, at low temperatures below 300 °C and high pressures above 15 atm, the performance of the methanation reaction is deteriorated owing to limitations in the reaction kinetics.

CO_2 hardly participates in the methanation reaction and remains in the product. Therefore, a reduced CO_2 amount in the feed gas improves the methanation reaction performance. When the synthesis gas from a coal gasifier is used directly after the purification process, low methanation performance is obtained owing to the deficient amount of H_2. An additional H_2 supply to the feed gas can increase the methanation performance significantly, and the optimal H_2/CO ratio appears to be about 3.

Through comparison of the equilibrium model calculations and dynamic numerical model simulations, both the thermodynamic equilibrium and reaction rate control the methanation reaction performance, especially in terms of the temperature and pressure. This work is expected to contribute to the optimal design and operation of the methanation reaction process for SNG production.

ACKNOWLEDGEMENTS

This research was supported by the Human Resources Development Program (20114010203050) of the Korea Institute of Energy Technology Evaluation and Planning (KETEP) grant funded by the Korean government Ministry of Trade, Industry and Energy and the National Agenda Program (NAP) of the Korea Research Council of Fundamental Science and Technology (KRCF).

NOMENCLATURE & ABBREVIATIONS

K_i : equilibrium constant of reaction i [i=1, 3, atm^{-2}; i=2, constant]
T : temperature [K]
Y_j : gas-phase mole fraction of component j
P : total pressure [atm]
α, β, γ : initial number of moles of CO, CO_2, and H_2 in methanation reactor [mol]
x : moles of reacted CO in reaction 1 [mol]
y : moles of reacted CO_2 in reaction 2 [mol]
$r_{i,j}$: rate of reaction i for component j [$mmol \cdot g^{-1} \cdot min^{-1}$]
k_i : rate constant of reaction i [i=1 and 3, $mmol \cdot atm^{1/2} \cdot g^{-1} \cdot min^{-1}$; i=2, $mmol \cdot g^{-1} \cdot min^{-1} \cdot atm^{-1}$]
p_j : partial pressure of component j
δ_j : surface adsorption parameter [atm^{-1}]
d_c : tube (column) inside diameter [cm]
A : tube (column) inside cross-sectional area [cm^2]
L_C : tube (column) length [cm]

ρ_b : bulk density of methanation catalyst [g·cm^{-3}]
C_{ps} : heat capacity of methanation catalyst [J·g^{-1}·K^{-1}]
ε : void fraction of methanation catalyst
T_w : outside tube wall temperature [K]
U_o : overall heat transfer coefficient [J·cm^{-2}·K^{-1}·min^{-1}]
t : time [min]
c_{pg} : heat capacity of gas phase [J·mmol^{-1}·K^{-1}]
ΔH_i : heat of reaction i [kJ·mol^{-1}]
N : total gas flux [mmol·cm^{-2}·min^{-1}]
n_t : total number of moles in gas phase [mmol·min^{-1}]
L_{stage} : length of CSTR stage [cm]
V_{stage} : volume of CSTR stage [cm^3]
R : gas constant [atm·cm^3·mmol^{-1}·K^{-1}]
η : factor for heat capacity of the heat exchanger tube and body
t_b : breakthrough time
SNG : synthetic natural gas
CSTRs : continuous stirred tank reactors

REFERENCES

1. P. Mondal, G. S. Dang and M. O. Garg, *Fuel Process Technol*., **92**, 1395 (2011).
2. J. H. Choi, Y. C. Bak, H. J. Jang, J. F. Kim and J. H. Kim, *Korean J. Chem. Eng*., **21**, 726 (2004).
3. S. Y. Chen, W. G. Xiang, D. Wang and Z. P. Xue, *Appl. Energy*, **95**, 285 (2012).
4. M. Hook and K. Aleklett, *Int. J. Energy Res*., **34**, 848 (2010).
5. B. Chen, X. Y. Wei, Z. M. Zong, Z. S. Yang, Y. Qing and C. Liu, *Appl. Energy*, **88**, 4570 (2011).
6. S. Shafiee and E. Topal, *Appl. Energy*, **87**, 988 (2010).
7. IEA, *World energy outlook 2011 special report*, International Energy Agency, Paris (2011).
8. J. Kopyscinski, T. J. Schildhauer and S. M. A. Biollaz, *Fuel*, **89**, 1763 (2010).
9. S. Ariyapadi, P. Shires, M. Bhargava and D. Ebbern, *Twenty-fifth annual international pittsburgh coal conference*, Pittsburgh, USA (2008).
10. D. A. Bell, B. F. Towler and M. Fan, *Coal gasification and its applications*, Elsevier, Oxford (2011).
11. K. H. Eisenlohr, F. W. Moeller and M. E. Dry, *A.C.S. Fuel*, **19**, 1 (1974).
12. J. E. Landers, *Sixth synthetic pipeline gas symposium*, Chicago, USA (1974).
13. R. L. Ensell and H. J. F. Stroud, *International gas research conference*, London, UK (1983).
14. R. Harth, W. Jansing and H. Teubner, *Nuclear Eng. Design.*, **121**, 173 (1990).
15. G. A. White, T. R. Roszkows and D. W. Stanbrid, *A.C.S. Fuel*, **19**, 57 (1974).
16. J. R. Rostrup-Nielsen, K. Pedersen and J. Sehested, *Appl. Catal. A-Gen*., **330**, 134 (2007).
17. G. Energy, Hydromethanation, GreatPoint Energy, Cambridge, USA (2009).
18. E. Everitt, D. C. Cicero and G. J. Stiegel, *Co-production of substitute natural gas/electricity via catalytic coal gasification*, National Energy Technology Laboratory, USA (2009).
19. G. J. Stiegel, *Overview of DOEs gasification program*, National Energy Technology Laboratory, USA (2009).
20. D. C. Cicero, G. J. Stiegel and E. Everitt, *Development of a hydrogasification process for co-production of substitute natural gas (SNG) and electric power from western coals*, National Energy Technology Laboratory, USA (2009).
21. I. Aigner, C. Pfeifer and H. Hofbauer, *Fuel*, **90**, 2404 (2011).
22. A. Duret, C. Friedli and F. Marechal, *J. Clean. Prod*., **13**, 1434 (2005).
23. M. C. Seemann, T. J. Schildhauer and S. M. A. Biollaz, *Ind. Eng. Chem. Res*., **49**, 7034 (2010).
24. T. Grobl, H. Walter and M. Haider, *Appl. Energy*, **97**, 451 (2012).
25. J. P. Strakey, A. J. Forney and W. P. Haynes, *Methanation in coal gasification processes*, Pittsburgh Energy Research Center, Pittsburgh (1975).
26. M. V. Twigg, *Catalyst handbook*, 2nd Ed., Wolfe Publishing Co., London (1989).
27. J. G. Xu and G. F. Froment, *AIChE J*., **35**, 88 (1989).
28. F. Gallucci, L. Paturzo and A. Basile, *Int. J. Hydrog. Energy*, **29**, 611 (2004).
29. Z. B. Rui, K. Zhang, Y. D. Li and Y. S. Lin, *Int. J. Hydrog. Energy*, **33**, 2246 (2008).
30. M. Zanfir, A. Gavriilidis, *Chem. Eng. Sci*., **58**, 3947 (2003).
31. S. S. E. H. Eisenlohr and S. S. Elshishini, *Modeling, simulation and optimization of industrial fixed bed catalytic reactor*, 7th Ed., Gordon and Breach Science Publishers, New York (1993).
32. O. Levenspiel, *Chemical reaction engineering*, 3rd Ed., Wiley, New York (1999).
33. H. M. Jang, K. B. Lee, H. S. Caram and S. Sircar, *Chem. Eng. Sci.*, **73**, 431 (2012).